Digest Journal of Nanomaterials and Biostructures Vol. 17, No. 4, October-December 2022, p. 1511-1526

# Preparation and properties of Ag-loaded zinc oxide antibacterial coating on medical cobalt-chromium alloy

X. P. Xu, Y. Q. Cai*, X. G. Chen, Y. Xu
*College of Materials Science and Engineering, North China University of Science and Technology, Tangshan 063210, Hebei, PR China*

Medical cobalt-chromium alloy has been widely used in oral implants due to its excellent mechanical properties, corrosion resistance, etc. However, its antibacterial properties should be improved as an implant. In this paper, nano-zinc oxide and Ag-loaded zinc oxide coating were prepared on cobalt-chromium alloy using the hydrothermal and photoreduction methods, and the influencing factors of the preparation process were studied. The effects of pH, hydrothermal temperature and time on the morphology of nano-sized zinc oxide were investigated. The results show that the zinc oxide has satisfactory morphology when the hydrothermal time is 3.0 h, hydrothermal temperature is 100 ℃, and pH value is 9.5. The effects of light intensity, illumination duration and $AgNO_3$ concentration on the size and dispersion of silver nanoparticles on the Ag-loaded zinc oxide were studied. The results show that the Ag-loaded zinc oxide has satisfactory morphology under the illumination intensity of 0.6 W/m$^2$, illumination duration of 60 min and $AgNO_3$ concentration of 1.0 mol/L. By analyzing the morphology, phase, quality and thickness of zinc oxide and Ag-loaded zinc oxide coating, it is found that the needle-like zinc oxide array is uniformly loaded with silver particles. The average thickness of the coatings is 6.80 μm, and the average weight is 1.67 mg. The antibacterial test shows that the Ag-loaded zinc oxide coating has better antibacterial performance than the pure zinc oxide coating, both of which were better than the blank control sample.

(Received June 26, 2022; December 19, 2022)

*Keywords*: Hydrothermal method, Photoreduction, Ag-loaded nano-zinc oxide, Antibacterial coating

## 1. Introduction

Cobalt-chromium alloys have good biological properties, high corrosion resistance, wear-resistance and strength, and are widely used in the manufacturing of implants and various medical devices[1-4]. However, the surface of cobalt-chromium alloy is easy to breed bacteria, and there are many limitations in drug immersion and disinfection. Silver ions have good thermal stability, strong and lasting antibacterial effect, and the preparation of Ag-loaded coatings to resist bacterial infection has become a research focus. As an inorganic antibacterial agent, zinc oxide has an excellent antibacterial effect on almost all cell strains. Although the antibacterial activity of zinc

* Corresponding author: caiyanqing126@126.com
https://doi.org/10.15251/DJNB.2022.174.1511

oxide is not as good as silver, the lower cytotoxicity and better biocompatibility are favored by researchers. The Ag-loaded zinc oxide composite coating[5-7] combines the advantages of silver and zinc oxide, and the synergistic antibacterial effect of the two further improves the antibacterial performance of inorganic antibacterial materials, which not only reduces the amount of silver, but also improves the antibacterial effect and significantly reduced cytotoxic effects caused by excess silver [8-10]. At the same time, due to its rich surface morphology [11, 12], nano-zinc oxide makes silver more stable, reduces the aggregation of silver nanoparticles, makes silver better dispersibility, and dramatically improves its antibacterial efficiency.

The preparation methods of zinc oxide mainly include sol-gel method [13], hydrothermal method[14-16], precipitation method [17, 18], vapor deposition method[19] and magnetron sputtering method[20]. Nanoparticles prepared by the hydrothermal method have uniform dispersion, high purity, good and controllable crystal shape, and low production cost. There is no sintering process when preparing nanomaterials by the hydrothermal method, so there is no need to worry about the influence of grain growth and the introduction of impurities in the sintering step. Tuo et al.[21] first prepared nano-zinc oxide by precipitation method, and then carried silver on nano-zinc oxide by pyrolysis method. The particle size of the prepared Ag-loaded zinc oxide composite nanoparticles was 192 nm. Duan et al.[22] used precursor thermal decomposition to uniformly deposit Ag on the surface of ZnO to prepare Ag/ZnO composite nanoparticles. Wu Dan [23] firstly prepared nano-ZnO powder by direct precipitation, and then Ag/ZnO nanocomposites were prepared by the PVP reduction and interface method.

In the present paper, ZnO nanorods were first prepared on a cobalt-chromium alloy substrate by the hydrothermal method, and then the ZnO was loaded with silver by a photoreduction method. The effects of different experimental conditions on the morphology of ZnO nanorods and the dispersion of silver nanoparticles were studied, and the nano-ZnO and Ag-loaded ZnO coatings were characterized by XRD, SEM, etc.

## 2. Experimental

### 2.1. Materials and methods

Cobalt-chromium alloy was obtained from Chengxin Rare Metal Products Co., Ltd. (Taobao, China), zinc acetate dihydrate, zinc nitrate hexahydrate, hexamethylenetetramine, silver nitrate, acetone, concentrated sulfuric acid, and absolute ethanol were analytically pure and obtained from Oerlikon Metco (Winterthur, Switzerland).

The X-ray diffraction (XRD) patterns were obtained on D/MAX2500PC (Japan). The fractured surface morphology of the coatings was observed by scanning electron microscopy (S4800, Hitachi). An ultraviolet photoreactor (PL-DY1600) was used for photoreduction to prepare silver particles (Taobao, China). The electronic balance and electronic digital micrometer were used to measure the quality and thickness of the coatings.

### 2.2. Preparation of nano-zinc oxide

The sample was pretreated as follows: the surface of the cobalt-chromium alloy was polished with sandpaper, and then the alloy sheet was cleaned with acetone or absolute ethanol. 50 mL of deionized water in the beaker was measure, and then 1.25 mL of concentrated sulfuric acid

and 3.75 mL of concentrated hydrochloric acid were poured into the beaker. The sample was put into the beaker, standed for 5 minutes, then was rinsed and dried.

0.2195 g of zinc acetate dihydrate was dissolved in 100 mL of deionized water to prepare a 0.01 mol/L zinc acetate dihydrate aqueous solution. The solution and samples were put into a hydrothermal kettle, and the hydrothermal kettle was placed in an oven at 100 °C for 1.0 h. A mixed solution of 0.025 mol/L zinc hexahydrate and 0.025 mol/L hexamethylenetetramine was prepared. The sample was taken out of the oven, put into the prepared mixed solution of zinc hexahydrate and hexamethylenetetramine, and heated in an oven at 100 °C for 3.0 h. The samples were taken out and dried in an oven at 85 °C for 30 min to obtain nano-zinc oxide.

### 2.3. Preparation of Ag-loaded zinc oxide

1.698 g of $AgNO_3$ was dissolved in 100 mL of deionized water, and then the nano-zinc oxide-loaded alloy was put into the $AgNO_3$ solution and irradiated with ultraviolet light for 1 h. Then Ag-loaded zinc oxide sample was obtained. The flow chart of the preparation of Ag-loaded zinc oxide is shown in Figure 1.

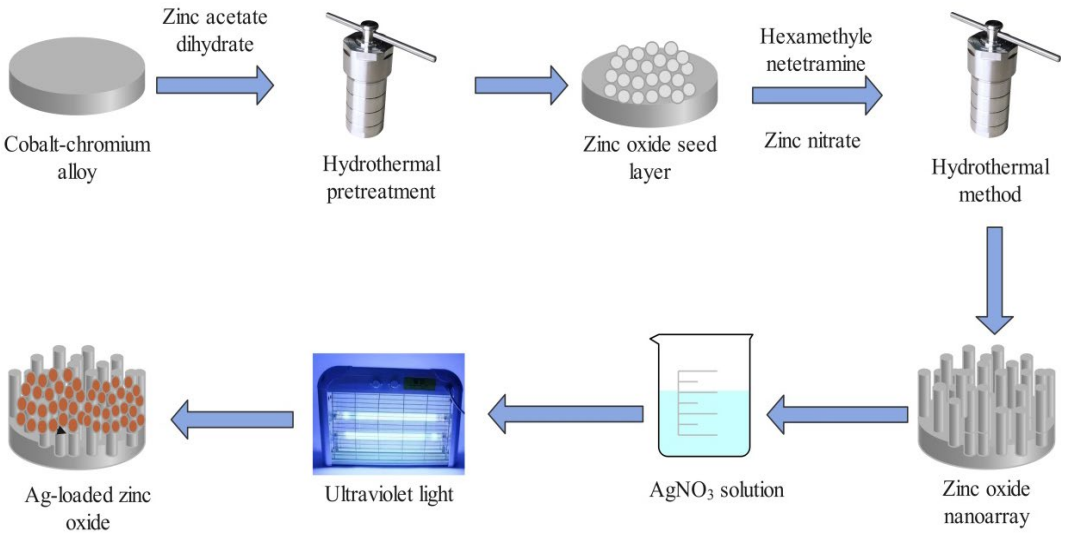


*Fig. 1. Preparation flow chart of Ag-loaded zinc oxide coating.*

## 3. Results and Discussion

### 3.1. Influence of preparation conditions on the morphology of nano-ZnO

#### *3.1.1. Effect of pH value on the morphology of nano-ZnO*

The pH value affects the solubility of the precursor, and can change the growth direction and process. Controlling suitable pH value is beneficial to the orientation growth of the crystal, and the structure, morphology and properties of the product will be different. In the present paper, $NH_3 \cdot H_2O$ was used as a pH adjuster to provide an alkaline environment, and it also acts as a complexing agent to form complexes with $Zn^{2+}$. Before adding $NH_3 \cdot H_2O$, the pH value of the solution was about 5.5, which was adjusted to 3.5 with hydrochloric acid firstly. Then the pH increased from 3.5 to 9.5 by changing the addition of $NH_3 \cdot H_2O$. The above reaction was shown in

Reaction (1), and the white precipitate $Zn(OH)_2$ appeared and increased. When $Zn^{2+}$ in the solution reacted after completion, $Zn(OH)_2$ is dissolved in $NH_3 \cdot H_2O$, and Reaction (2) occurs. When pH was 9.0, a large number of white $Zn(OH)_2$ particles and some $[Zn(NH_3)_4]^{2+}$ ions were produced. In the hydrothermal kettle, $Zn(OH)_2$ directly reacts to form ZnO, as shown in Reaction (3). And $[Zn(NH_3)_4]^{2+}$ reacts to form $[ZnO_2]^{2-}$and then ZnO crystals generates, as shown in Reaction (4).

$$Zn^{2+} + 2OH^- \rightarrow Zn(OH)_2 \quad (1)$$

$$Zn(OH)_2 + 4NH_3 \rightarrow [Zn(NH_3)_4]^{2+} + 2OH^- \quad (2)$$

$$Zn(OH)_2 \rightarrow ZnO\downarrow + H_2O \quad (3)$$

$$[Zn(NH_3)_4]^{2+} \rightarrow [ZnO_2]^{2-} \rightarrow ZnO\downarrow \quad (4)$$

Figure 2 shows the morphologies of nano-ZnO obtained at pH of 3.5, 5.5, 7.0, and 9.5, respectively.

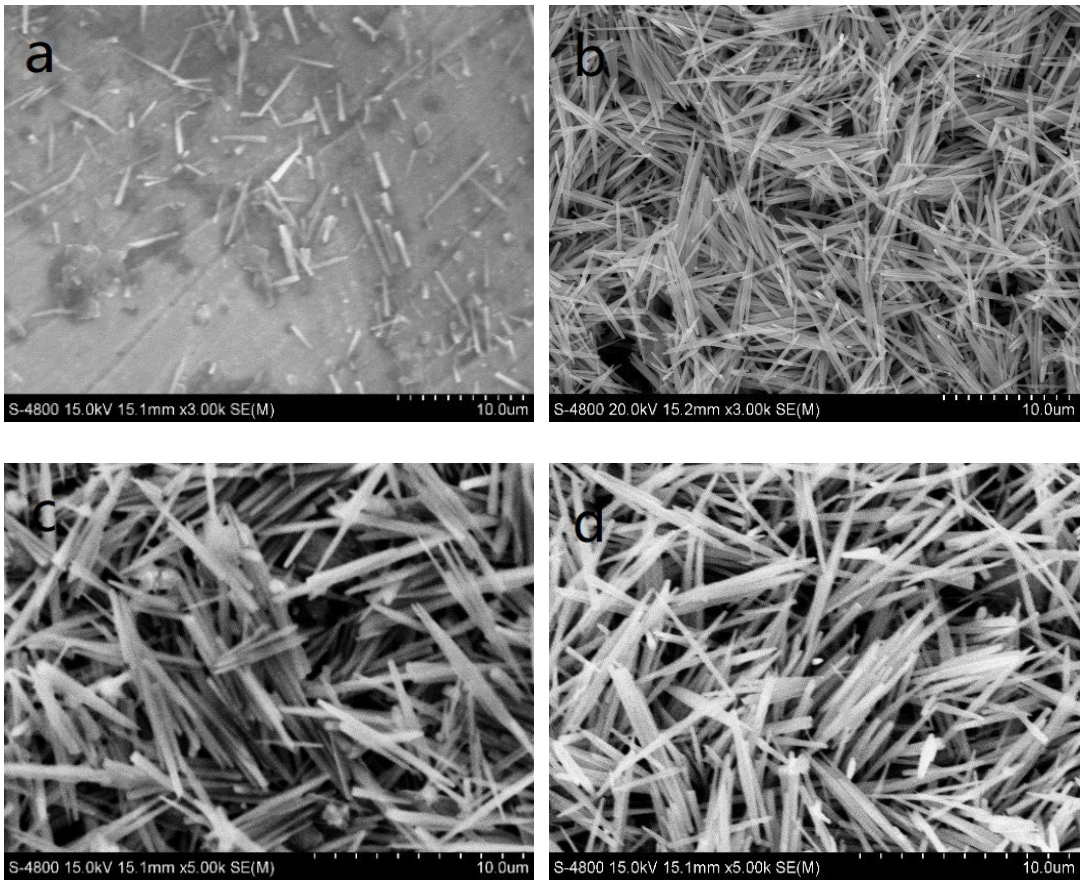


*Fig. 2. SEM images of nano-ZnO at different pH values (a) 3.5; (b) 5.5; (c) 7.0; (d) 9.5.*

As shown in Figure 2a, when the pH is 3.5, the growth of nano-ZnO is inhibited, and there is almost no crystal growth on the surface. When the pH is 5.5, it can be seen from Figure 2b that

ZnO is elongated needle-like, with a crystal length of 5~7 μm and a crystal diameter of 300 nm. When the pH increases to 7.0 and 9.5, the shapes of zinc oxides become long columns. At the same time, the aspect ratios decrease obviously, and the orientation is good. Therefore, when the pH is 9.5 and the solution is weakly alkaline, the morphology and orientation of nano-ZnO are better.

### *3.1.2. Effect of hydrothermal temperature on the morphology of nano-ZnO*

The control of hydrothermal temperature is significant important in the reaction process, which affects the reaction progress and crystallization speed, and also directly affects the growth process of nanocrystals. Furthermore, the morphology and properties of the products are also affected. Figure 3 shows the morphologies of the nano-ZnO obtained at hydrothermal temperatures of 90 ℃, 95 ℃, 100 ℃, and 110 ℃, respectively. As shown in Figure 3a, when the temperature is 90 °C, the zinc oxide is fine needle, the crystal length is about 5.0 μm, and the crystal diameter is 300 nm. It can be seen from Figures 3b and c that with the temperature of 95 ℃ and 100 ℃, the average crystal diameter has no noticeable change, but the crystal length increases. When the reaction temperature was 110 °C, the crystal length increased to 7 μm. Finally, the optimal reaction temperature is chosen as 100 °C.

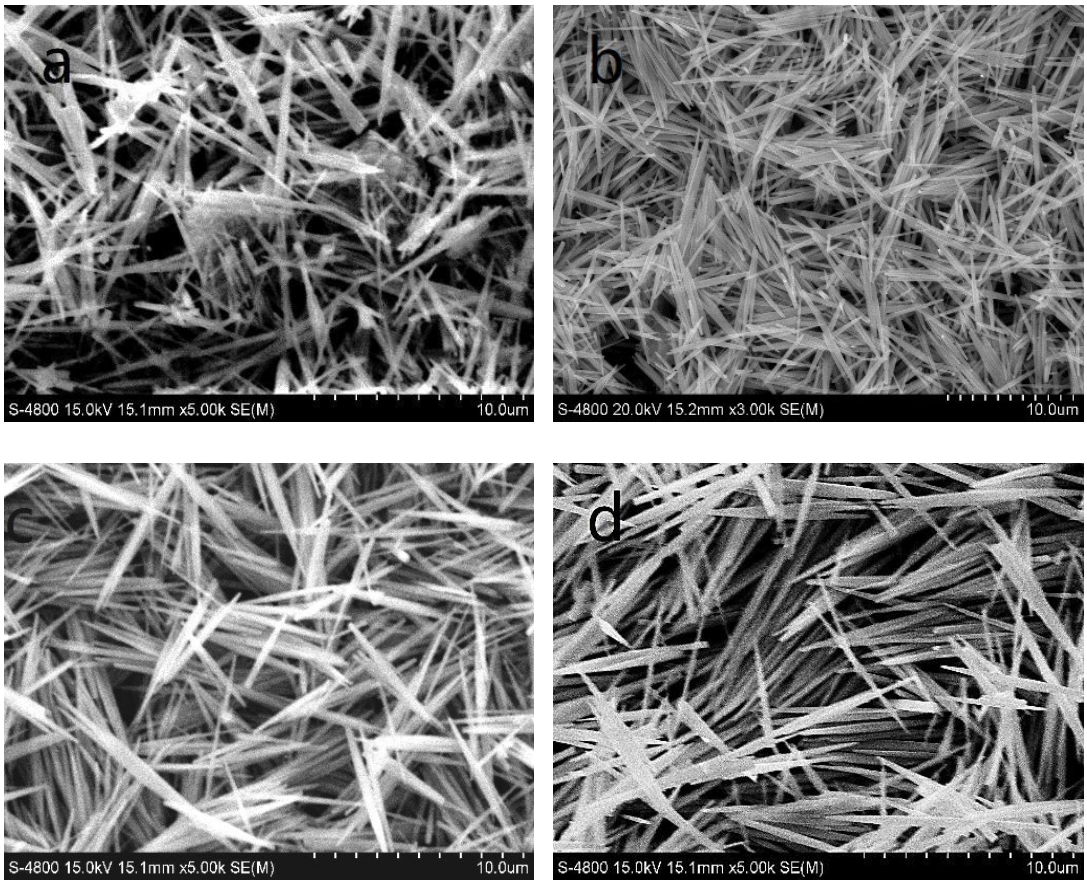


*Fig. 3. SEM images of nano-ZnO at different temperatures (a) 90 ℃; (b) 95 ℃; (c) 100 ℃; (d) 110 ℃.*

### *3.1.3 Effect of reaction time on the morphology of nano-ZnO*

Reaction time also has an impact on the morphology of the crystal. Under hydrothermal conditions, many ZnO nanoparticles were firstly formed on the substrate after 1.0 h of hydrothermal pretreatment, which provided nuclei for the growth of ZnO nanorods. These nuclei randomly grew on the cobalt-chromium substrate, and ZnO nanoparticles started to grow based on these nuclei. As time went on, the length and diameter of ZnO crystals increased in turn, while when the time continued to increase, the crystals stopped growing.

Figure 4(a~d) shows the morphologies of nano-ZnO obtained under the reaction time of 1 h, 3 h, 4 h, and 5 h, respectively. As shown in Figure 4a, when the reaction time is 1 h, the zinc oxide crystals are not fully grown due to the short reaction time, the surface crystals are sparse and short in length, the crystal length is 2~3 μm, and the average crystal diameter is about 200 nm. It can be seen from Figure 4b that when the reaction time is 3 h, the oxygen crystals grow to be slender needles with a crystal length of 6~7 μm and an average crystal diameter of 300 nm. As shown in Figure 4c~d, as the reaction time increases, ZnO continues to grow, the crystal length increases, and the crystal diameter becomes finer. Therefore, the optimal reaction time can be controlled at 3h to prepare nano-ZnO.

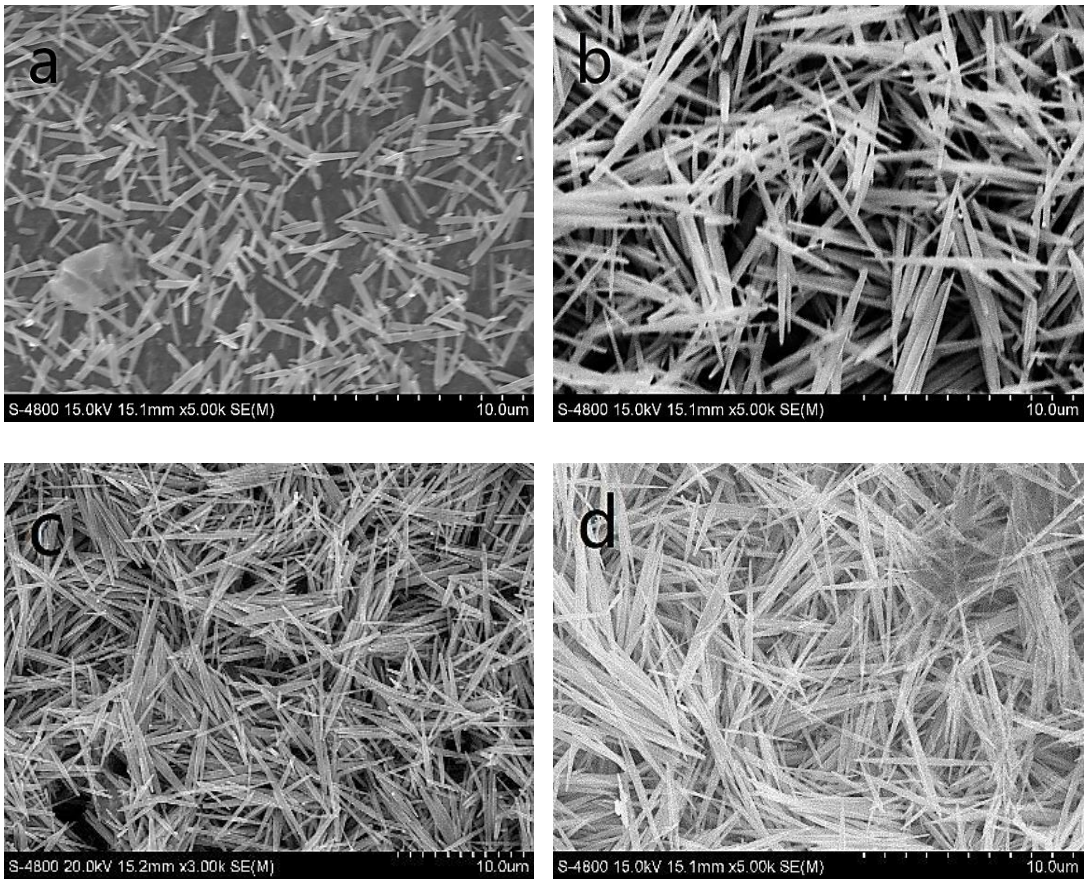


*Fig. 4. SEM images of nano-ZnO obtained at different times (a) 1 h; (b) 3 h; (c) 4 h; (d) 5 h.*

### *3.1.4. Morphology and composition of nano-ZnO prepared under optimal conditions*

For the above optimal conditions, nano-ZnO was prepared under the hydrothermal time of 3 h, hydrothermal temperature of 100 °C, and pH of 9.5. The surface morphology of the prepared nano-ZnO and composition of needles in the photo were detected, as shown in Figure 5.

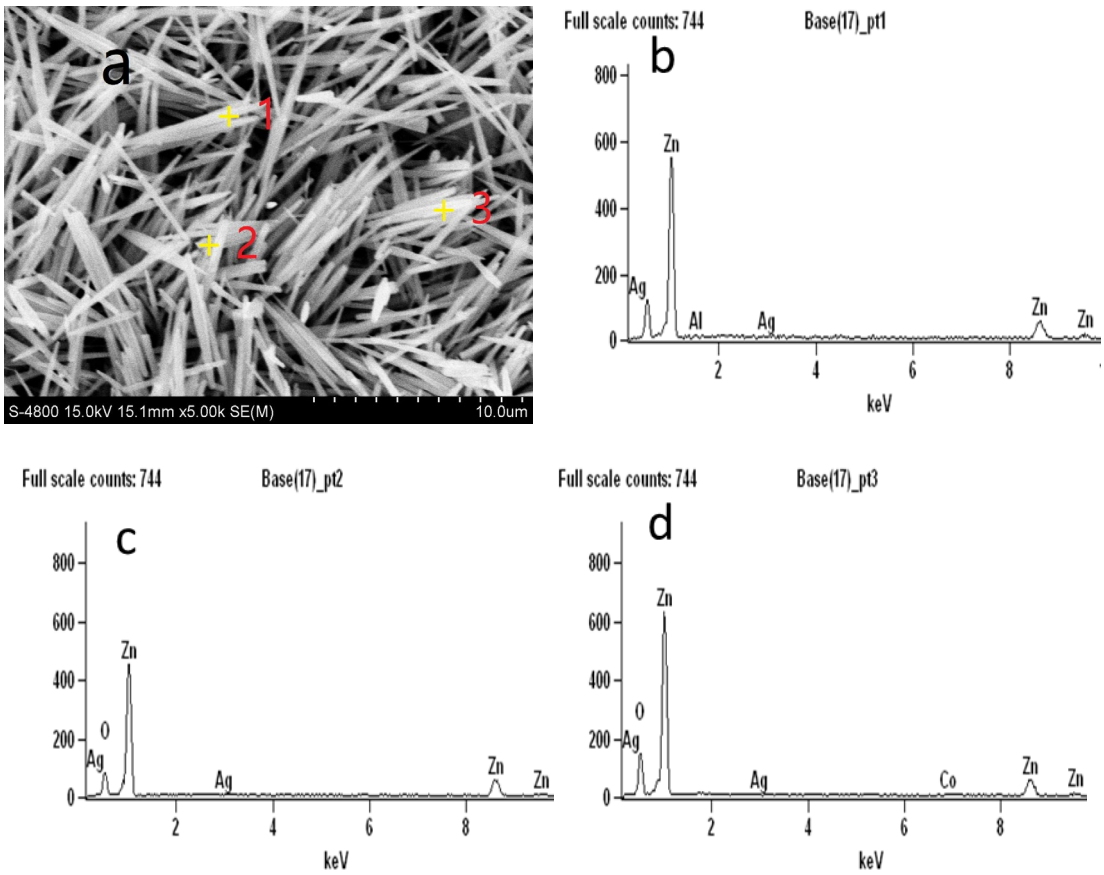


*Fig. 5. (a)SEM image of Nano-Zinc Oxide and (b~d) 1, 2, 3 point scanning.*

According to the SEM image and EDS analysis in Figure 5, it can be seen that the nano-zinc oxide has good crystallinity. The average crystal length is 7 μm, the average crystal diameter is 300 nm, and the crystal is fine needle-like. The EDS analyses of specific points 1, 2, and 3 show that the surface of the cobalt-chromium alloy was mainly nano-zinc oxide and the zinc oxide crystal arrays are very dense.

## 3.2. Influencing factors on the morphology of Ag-loaded ZnO

### *3.2.1. Effect of light intensity on the morphology of Ag-loaded zinc oxide*

Figure 6 shows the SEM images of the Ag-loaded ZnO samples obtained under different light intensities in 1.0 mol/L $AgNO_3$ for 10 min. It can be seen from Figure 6 that $AgNO_3$ undergoes a photoreduction reaction under certain light intensity, and the surface of nano-zinc oxide is loaded with nano-silver particles. However, the light intensity will influence the photoreduction reaction and affect the electroless silver particles. When the light intensity is 0.4 $W/m^2$, the activation energy is low, and the photoreduction reaction cannot proceed. It can be seen

from Figure 6a that the reaction hardly proceeds and silver does not appear. When the light intensity is 0.6 W/m$^2$, the activation energy is sufficient and the reaction is fully carried out. It can be seen from Figure 6b that there are many silver nanoparticles with good dispersibility. The obtained silver nanoparticles have an average diameter of 300 nm and are attached to each zinc oxide crystal. However, when the light intensity is 0.8 W/m$^2$, the number of nano-silver particles decreases sharply, indicating that high light intensity may be unfavorable for the photoreduction reaction. In summary, under a series of light intensities of 0.4 W/m$^2$, 0.6 W/m$^2$, and 0.8 W/m$^2$, the optimal light intensity can be controlled to 0.6 W/m$^2$.

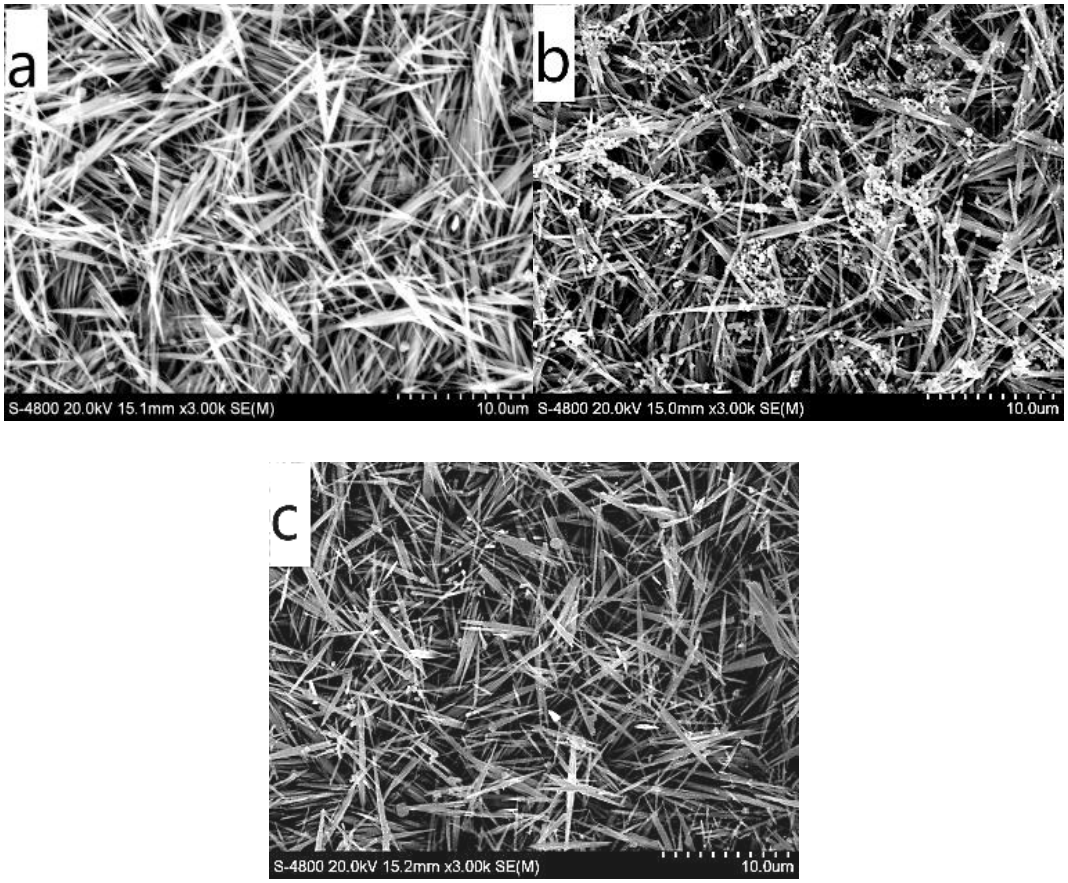


*Fig. 6. SEM images of Ag-loaded zinc oxide under different light intensity (a) 0.4 W /m$^2$; (b) 0.6 W/m$^2$; (c) 0.8 W/m$^2$.*

### *3.2.2. Effect of illumination duration on the morphology of Ag-loaded ZnO*

Although illumination duration is not as decisive as illumination intensity, it still affects the progress of photoreduction reaction. Figure 7 shows the SEM images of the samples obtained under different illumination durations, with 1.0 mol/L $AgNO_3$ and illumination intensity of 0.6 W/m$^2$. The surface of nano-zinc oxide in Figure 7a is loaded with nano-silver particles, and the diameter of the obtained nano-silver particles is about 200 nm. From Figure 7b, when the illumination duration is 30 min, the generated nano-silver particles are more significant and agglomeration occurs. From Figure 7c that when the illumination duration is 60 min, the

nano-silver particles are more uniform, and there is no reunion phenomenon. In general, the illumination time has little effect on the formation of nano-silver, and the best illumination duration can be chosen as 60 min.

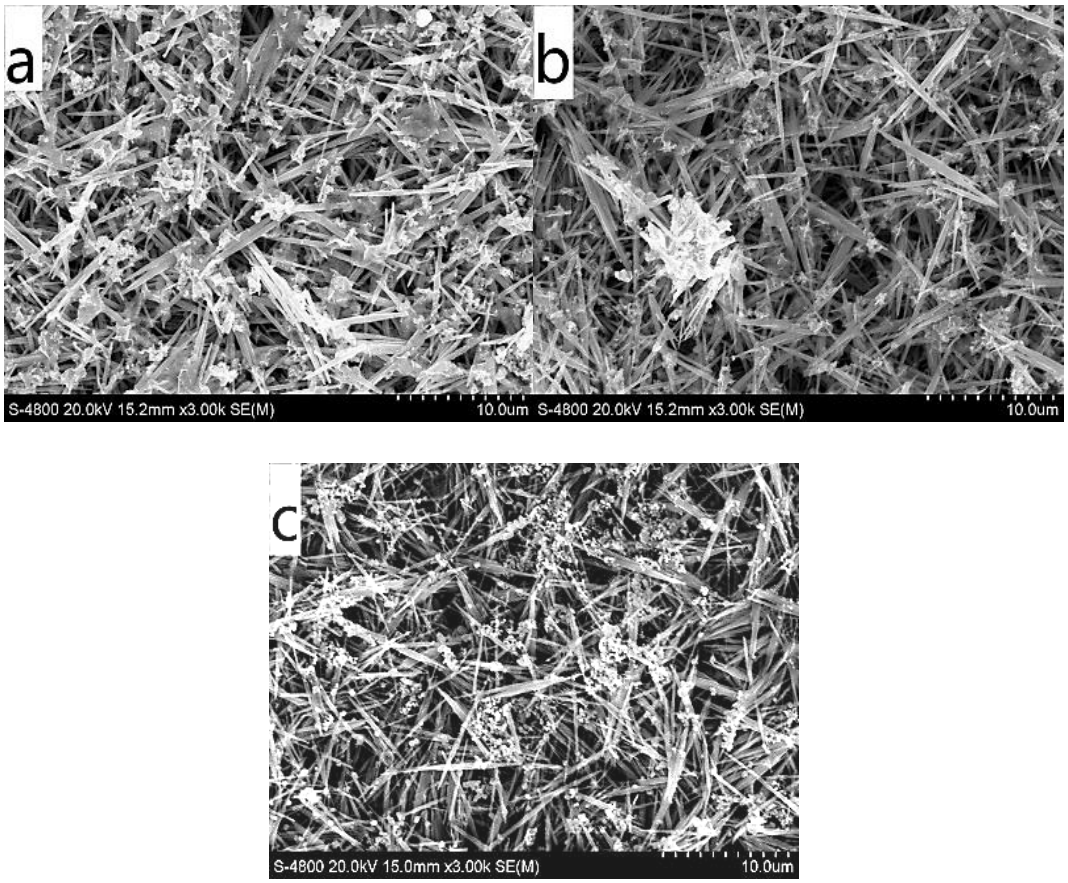


*Fig. 7. SEM images of Ag-loaded zinc oxide under different illumination durations (a) 10 min; (b)30 min; (c)60 min.*

### *3.2.3. Effect of $AgNO_3$ concentration on the morphology of Ag-loaded ZnO*

Figure 8 shows the SEM images of the samples obtained under different $AgNO_3$ concentrations, with the illumination duration of 60 min and the light intensity of 0.6 W/m$^2$. It can be seen from Figure 8a that when the $AgNO_3$ concentration is 0.3 mol/L, fewer nano-silver particles are formed. The silver particles cannot be attached to the zinc oxide crystal, and the dispersibility is poor. As seen from Figure 8b, when the concentration is 0.6 mol/L, the generated nano-silver particles are improved, the particle diameter is about 1.5 μm, and the dispersibility is better. It can be seen from Figure 8c that when the $AgNO_3$ concentration is 1.0 mol/L, the reaction degree is good. The nano-silver particles are attached to the ZnO crystal and have good dispersibility without agglomeration phenomenon, and the particle diameter is about 200 nm. Thus the optimum $AgNO_3$ concentration can be chosen as 1.0 mol/L.

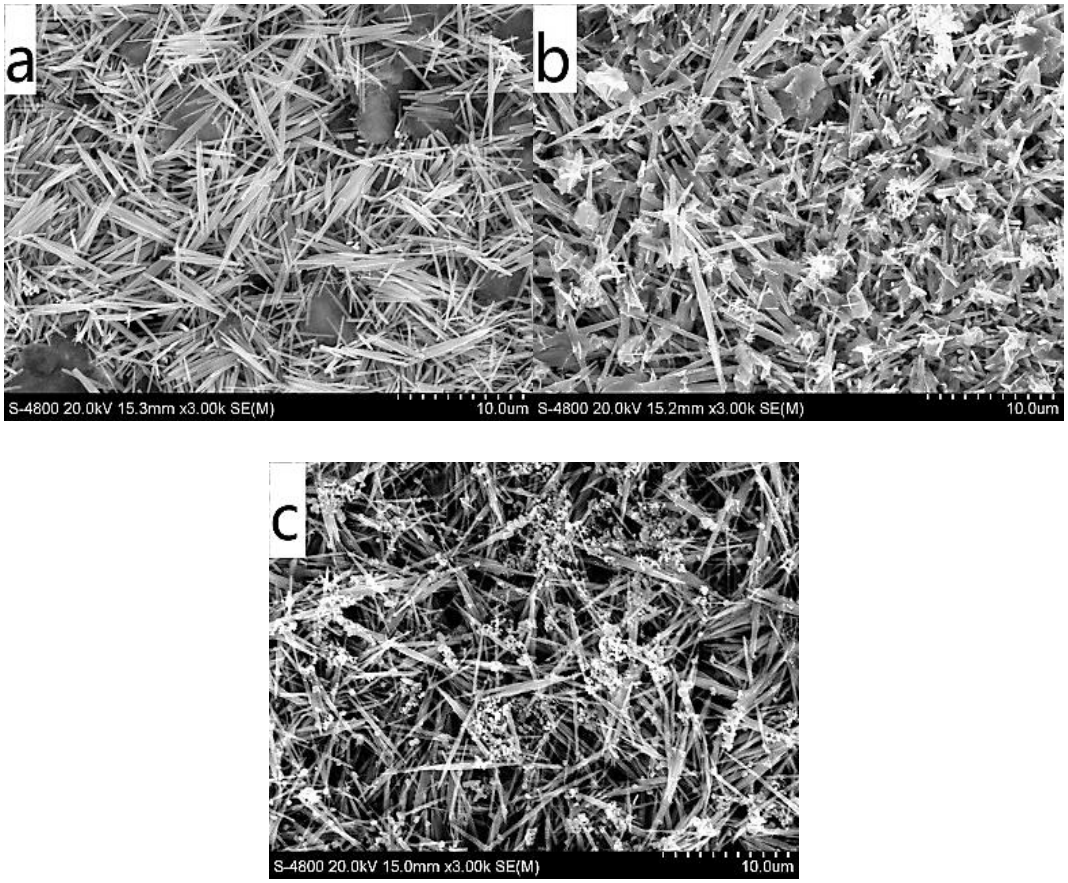


*Fig. 8. SEM images of Ag-loaded zinc oxide with different $AgNO_3$ concentrations (a) 0.3 mol/L; (b) 0.6 mol/L; (c) 1.0 mol/L.*

### *3.2.4. Morphology and EDS analyses of Ag-loaded zinc oxide coating obtained under optimal conditions*

Ag-loaded zinc oxide coating was prepared under the optimal conditions, such as the hydrothermal time was 3.0 h, the hydrothermal temperature was 100 ℃, the pH was 9.5, the light intensity was 0.6 $W/m^2$, the illumination duration was 60 min, and the $AgNO_3$ concentration was 1.0 mol/L. After that, the surface morphology and EDS analyses of the Ag-loaded zinc oxide coating are performed, as shown in Figure 9.

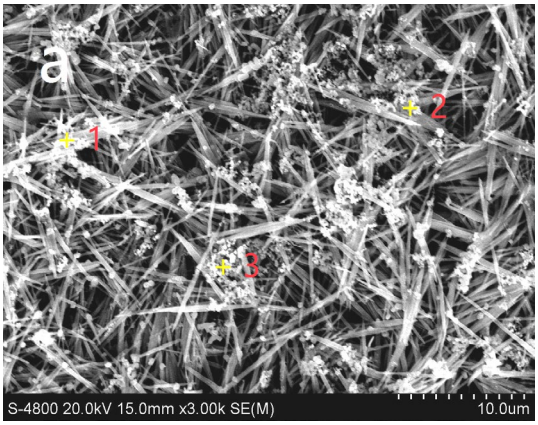
a
1
2
3
S-4800 20.0kV 15.0mm x3.00k SE(M)
10.0um

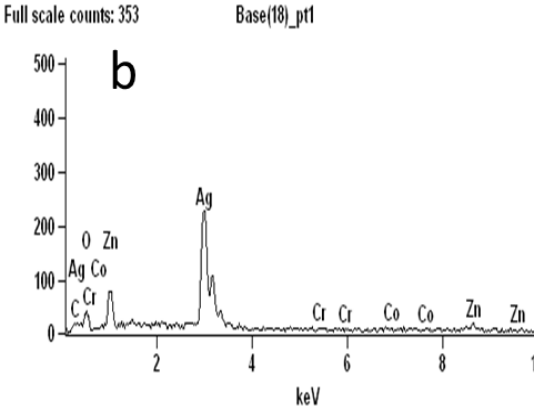
Full scale counts: 353
Base(18)_pt1
b
Ag
O Zn
Ag Co
Cr
C
Cr Cr Co Co Zn Zn
keV

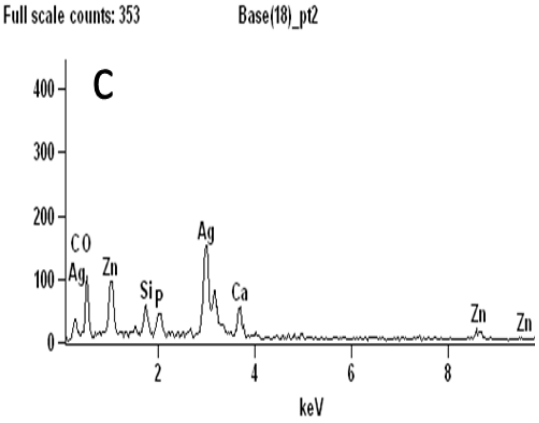
Full scale counts: 353
Base(18)_pt2
c
CO
Ag
Zn
Si P
Ag
Ca
Zn Zn
keV

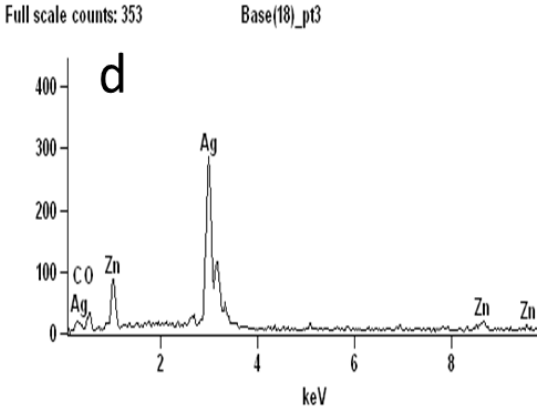
Full scale counts: 353
Base(18)_pt3
d
Ag
CO
Ag
Zn
Zn Zn
keV

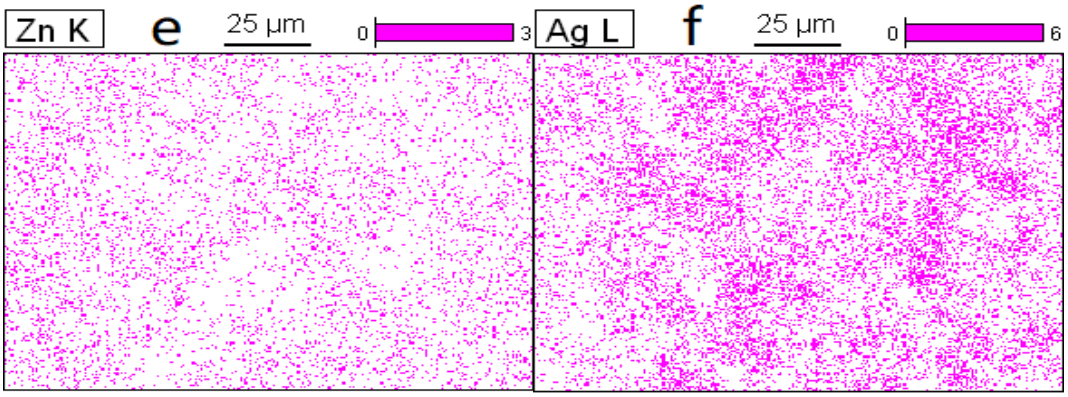
Zn K
e
25 µm
0
3
Ag L
f
25 µm
0
6

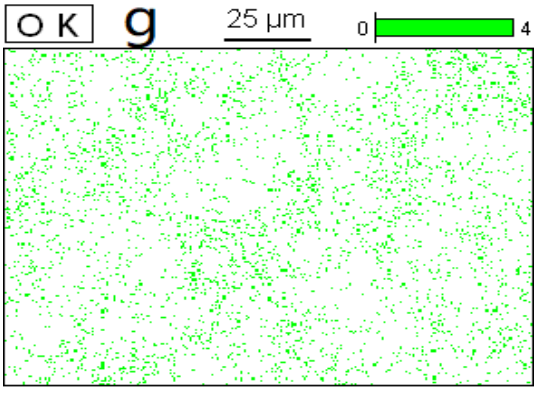
O K
g
25 µm
0
4

*Fig. 9. (a)SEM image of Ag-loaded zinc oxide, (b~d)1,2,3 point scanning, and (e~g) area mapping of (a).*

From the SEM image in Figure 9a, it can be seen that nano-silver particles are attached to each ZnO crystal and have good dispersibility. The obtained nano-silver particles are about 200 nm in diameter. From the EDS analyses, when the selected point is on the nano-silver particles, the silver content is higher, while Zn and O are lower.

According to the mapping results, it can be seen from Figure 9f that the nano-silver particles are uniformly dispersed and loaded on the zinc oxide crystal. The mapping analysis did not detect the cobalt-chromium matrix, which proves that the surface of the cobalt-chromium alloy is modified and loaded with a tight Ag-loaded zinc oxide coating.

### 3.3. XRD analyses of zinc oxide and Ag-loaded zinc oxide coatings

XRD analyses of zinc oxide and Ag-loaded zinc oxide coatings obtained under optimal conditions were conducted, as shown in Figure 10.

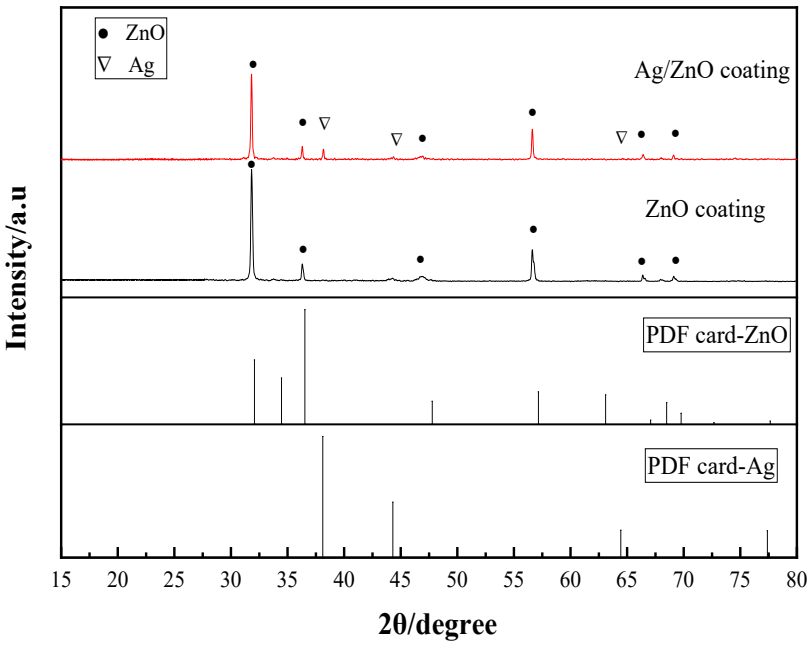


*Fig. 10. XRD patterns of zinc oxide and Ag-loaded zinc oxide coatings.*

As shown in Figure 10, the diffraction peaks of zinc oxide are consistent with the standard card of ZnO (JCPDS No. 99-0111), and the 2θ angle at 31.766°, 34.418°, 36.251°, 47.535°, 56.591°, 62.851°, 66.371°, 67.942° and 69.081° are corresponding to (100), (002), (101), (102), (110), (103), (200), (112) and (201) crystal planes, respectively. Moreover, diffraction peaks appear at 38.116°, 44.277° and 64.426° were in line with the characteristic diffraction peaks of the standard PDF card of Ag (JCPDS. No.04-0783), corresponding to the (111), (200) and (220) crystal planes, respectively. It proves that zinc oxide and Ag-loaded zinc oxide coatings were successfully prepared. The crystal structure of zinc oxide is a hexagonal wurtzite structure. The diffraction peaks in Figure 10 are sharp and narrow, indicating the crystallinity of the sample is well, with high purity and no impurities.

### 3.4. Thickness and quality analyses of Ag-loaded zinc oxide coating

#### *3.4.1. Thickness analysis*

The thickness of the samples before and after loading the Ag-loaded zinc oxide coating under the optimal conditions was measured and recorded, respectively, and the results are shown in Table 1. For accuracy, each test was performed six times and the thickness was averaged. It can be seen that the average thickness change of the samples before and after loading the antibacterial coating is 6.80 μm.

*Table 1. Thickness changes of the samples.*

| No. | Before(mm) | After(mm) | Thickness(μm) | Average(μm) |
|---|---|---|---|---|
| 1 | 0.891 | 0.899 | 8.00 | 6.80 |
| 2 | 0.880 | 0.886 | 6.00 | |
| 3 | 0.874 | 0.881 | 7.00 | |
| 4 | 0.894 | 0.900 | 6.00 | |
| 5 | 0.898 | 0.905 | 7.00 | |
| 6 | 0.874 | 0.881 | 7.00 | |

#### *3.4.2. Quality Analysis*

The quality of the samples before and after loading the Ag-loaded zinc oxide coating under the optimal conditions was measured and recorded, and the results are shown in Table 2. For accuracy, each test was performed six times and the quality was averaged. It shows that the weight of the sample after loading the coating increases by 1.0 to 2.0 mg, with an average increase of 1.67 mg.

*Table 2. Quality changes of the samples.*

| No. | Before(g) | After(g) | Quality(mg) | Average(mg) |
|---|---|---|---|---|
| 1 | 0.142 | 0.143 | 1.0 | 1.67 |
| 2 | 0.138 | 0.140 | 2.0 | |
| 3 | 0.144 | 0.146 | 2.0 | |
| 4 | 0.140 | 0.141 | 1.0 | |
| 5 | 0.141 | 0.143 | 2.0 | |
| 6 | 0.137 | 0.139 | 2.0 | |

### 3.5. Antibacterial performance test of Ag-loaded zinc oxide coating

In this experiment, the antibacterial performance was tested by the bactericidal test. Taking the blank sample as the control group, antibacterial properties of nano-zinc oxide and Ag-loaded zinc oxide coating were conducted, and the results after 24 h of antibacterial testing were observed

and analyzed, as shown in Figure 11.

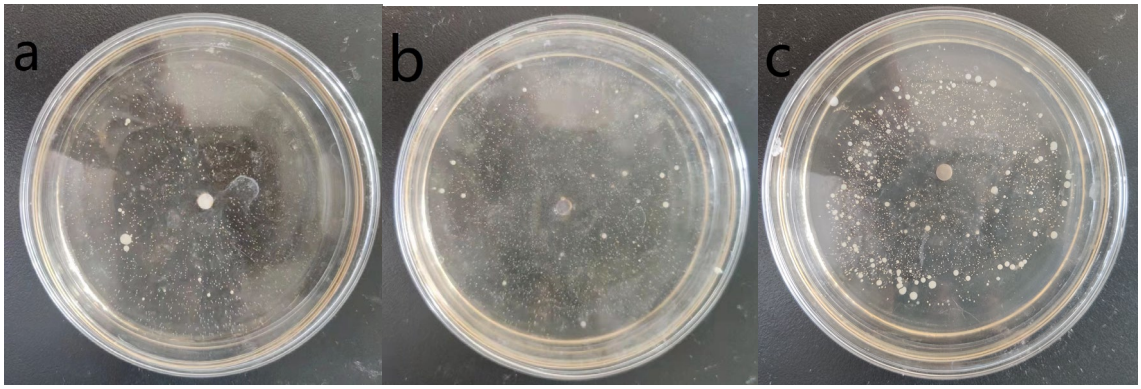


*Fig. 11. Antibacterial test photos of cobalt-chromium alloy surface layer (a: nano zinc oxide, b: Ag-loaded zinc oxide, c: blank).*

It can be seen from Figure 11a that there are fewer bacteria around the zinc oxide coating, and a small inhibition zone appears, which proves that zinc oxide has certain antibacterial properties. In Figure 11b, an expansive inhibition zone is formed with the Ag-loaded zinc oxide coating as the center, and the diameter of the inhibition zone is slightly larger than that in Figure 11a, which proves the antibacterial performance of Ag-loaded zinc oxide is better than that of zinc oxide. There are many bacteria around the sample in Figure 11c, and no inhibition zone is produced. In conclusion, the antibacterial properties of Ag-loaded zinc oxide are better than those of zinc oxide, but both are better than the blank sample.

## 4. Conclusion

In this paper, the antibacterial coating of zinc oxide and Ag-loaded zinc oxide was prepared by hydrothermal and photoreduction methods, and the influence of temperature, reaction time, pH, light intensity and other parameters on the preparation of nano-zinc oxide and Ag-loaded zinc oxide were investigated. The main conclusions are as follows.

(1) The optimal experimental scheme for preparing nano-zinc oxide is as follows, the hydrothermal time is 3 h, hydrothermal temperature is 100 ℃, and pH is 9.5. At the same time, the optimal scheme for preparing of Ag-loaded zinc oxide coating is that the light intensity is 0.6 $W/m^2$, illumination duration is 60 min, and $AgNO_3$ concentration is 1.0 mol /L.

(2) XRD analyses showed that both zinc oxide and Ag-loaded zinc oxide coatings were successfully prepared, and the crystal structure of zinc oxide was a hexagonal wurtzite structure. The coating quality and thickness results show that the coating has an average thickness of 6.80 μm and an average mass of 1.67 mg.

(3) SEM and EDS analyses show that nano-zinc oxide is fine needle-like and has good crystallinity. The average crystal length is 7.0 μm, the average crystal diameter is 300 nm. The obtained nano-silver particles are about 200 nm in diameter. The nano-silver particles are dispersed on the nano-zinc oxide, with good dispersibility and no accumulation, which improves

the stability of the Ag-loaded zinc oxide coating.

(4) The antibacterial test results show that both zinc oxide and Ag-loaded zinc oxide have antibacterial properties, and Ag-loaded zinc oxide has better antibacterial properties than zinc oxide, proving that Ag-loaded zinc oxide has better antibacterial properties than single-phase zinc oxide.

## Acknowledgements

The authors acknowledge the National University Student Innovation and Entrepreneurship Project (X2021028); Tangshan Science and Technology Plan Project (21130229C); North China University of Science and Technology Provincial University Fundamental Research Fund Project (JST2022005).

## References

[1]T. H. Wang , X. J. Cao. China Minkang Medicine 33(01),142(2021);

[2]H. J. Cai, Z. Liao, A. F. Zhang et al. Metal Functional Materials 27(02),28(2020);

[3]T. Jinno, V.M.Goldberg, D.Davy et al. Journal of Biomedical Materials Research 42(1),20(2015); https://doi.org/10.1002/(SICI)1097-4636(199810)42:1<20::AID-JBM4>3.0.CO;2-Q

[4] C. Chen, C.Yao, J. Yang et al. Colloids & Surfaces B Biointerfaces 151,156 (2017); https://doi.org/10.1016/j.colsurfb.2016.12.021

[5]H. Q. Bian, Z. M. Zhang, X. L. Xu et al. Physica, E. Low-dimensional systems & nanostructures, 124(2020); https://doi.org/10.1016/j.physe.2020.114236

[6]Z. Liu, T. Zhang, J. Shang. Chinese Journal of Experimental Surgery 35(07), 1383(2018);

[7]Q. Chen, Q. Wang, X. J. Wang et al. New Chemical Materials 48(06),134(2020);

[8] A.B. An , S.V. Shmakov, N.A. Verlov et al. Journal of Physics Conference Series 2086(1),012(2021);

[9]Z. Xiong, L.Liu, Z. Zhang et al. Toxicity Testing Alternative Methods and Translational Toxicology ( International) Academic Symposium, Shenyang, Liaoning,China, (2021);

[10]V. Bastos, J. M.P.Ferreira-De-Oliveira, J. Carrola et al. Journal of Environmental Sciences 51 (01),191(2017); https://doi.org/10.1016/j.jes.2016.05.028

[11]S. Bakhori, S. Mahmud, C. A. Ling et al. Materials science & engineering 78,868(2017); https://doi.org/10.1016/j.msec.2017.04.085

[12]H. Y. Liu, Y. Qiao-, B. Shi et al.China Agricultural Science and Technology Review 20(05),140(2018);

[13]R. Wang, Y. H. Sun, L. Huang et al. Journal of Synthetic Crystals 49(10), 1800(2020);

[14]S. Sathiya, J Vijayapriya, K Parasuraman et al. Journal of Metastable and Nanocrystalline Materials 32,33(2021); https://doi.org/10.4028/www.scientific.net/JMNM.32.33

[15]P. Khamkhom, M. Horprathum, S. Pokai et al. Materials Today: Proceedings 4(5), 6200(2017); https://doi.org/10.1016/j.matpr.2017.06.116

[16]M. Ajmi, K. Hamdi, M. S. Raad. Tikrit Journal of Pure Science 24(3), 91(2019); https://doi.org/10.25130/j.v24i3.822

[17]S. P. Xu. Guangdong Chemical Industry 47(19), 255(2020);

[18]Q. Q. Chen, L. M. Yang, W. Wang et al. Journal of Beijing Institute of Fashion Technology (Natural Science Edition) 39(01),46(2019);

[19]E. S. Babu, B. Saravanakumar, G. Ravi et al. Journal of Materials Science Materials in Electronics 29(8),6149(2018); https://doi.org/10.1007/s10854-018-8589-z

[20]J. K. Li, Y. A. Wang, H. B. Mu et al. Journal of Beijing Forestry University 41(01),119(2019);

[21]D. Tuo. Journal of Packaging 2(2),14(2010);

[22]X. Duan. Sichuan: Southwest Jiaotong University, (2012);

[23]D. Wu. Huazhong University of Science and Technology, (2013);